

SHEAR STRENGTH OF HDPE GEOMEMBRANE/GCL INTERFACES

The attached paper presents the results of interface shear strength tests between a standard needlepunch-reinforced woven/nonwoven GCL (Bentomat ST) and both smooth and textured HDPE geomembranes. Tests were performed in a large-scale direct shear machine capable of measuring peak and large displacement (200 mm) shear strengths. The failure surface was located at the GM/GCL interface for all tests, spanning normal stresses from 1 to 486 kPa (20 to 10,000 psf). None of the GCL samples failed internally during shearing. GCL interfaces with the smooth geomembranes showed the lowest peak shear strength (and smallest decrease in post-peak strength), while GCL interfaces with textured geomembranes showed the highest peak shear strength (and highest decrease in post-peak strength). Interface shear strengths for textured geomembranes placed against the nonwoven side of Bentomat ST were higher than those corresponding to the woven side. Damage mechanisms for geomembranes involve polishing and removal of asperities, while GCL damage mechanisms involve polishing, breakage, pullout, and alignment of geotextile fibers. Limited tests showed that peak and large displacement shear strengths were independent of displacement rate. The quantity of bentonite extrusion generally increased with increasing normal stress and was less for nonwoven geotextiles than for woven geotextiles. A two-stage hydration and consolidation procedure was effective in minimizing porewater pressure within 48 hours for up to 10,000 psf normal loads.

Shear strength information presented in this paper may be useful for gaining insight into GM/GCL interface behavior, and for preliminary design purposes. However, design values of GM/GCL interface shear strength should be measured on a project-specific basis under conditions similar to those expected in the field. The hydration-consolidation procedure presented in this paper is recommended for project direct shear testing.

SHEAR STRENGTH OF HDPE GEOMEMBRANE/GEOSYNTHETIC CLAY LINER INTERFACES

By Eric J. Triplett¹ and Patrick J. Fox,² Associate Members, ASCE

ABSTRACT: A study of interface shear strengths between smooth and textured high density polyethylene (HDPE) geomembranes (GMs) and a woven/nonwoven needle-punched geosynthetic clay liner (GCL) is presented. Tests were performed using a large direct shear machine capable of measuring peak and large displacement (200 mm) shear strengths. The failure surface was located at the GM/GCL interface for all tests conducted, corresponding to a normal stress range of 1–486 kPa. Small positive pore pressures were measured for all interfaces at peak shear strength. Thus, the practice of preparing failure envelopes using total normal stress, instead of effective normal stress, appears to be conservative. Interface shear strengths for textured GMs placed against the nonwoven side of the GCL were higher than those corresponding to the woven side. By comparison, differences in peak shear strength for laminated and coextruded GM interfaces were relatively less. Limited tests showed that peak and large displacement shear strengths were independent of displacement rate and dependent on the shear direction of the GM. The quantity of extruded bentonite at the interfaces generally increased with normal stress and was less for nonwoven geotextile interfaces than for woven geotextile interfaces. Implications of the findings to the testing of GM/GCL interfaces and the characterization of GM/GCL interface shear strength are discussed.

INTRODUCTION

The majority of geosynthetic clay liners (GCLs) are placed beneath geomembranes (GMs) to act as composite liners within landfill bottom liner and cover systems. Since these applications typically involve side slopes, stability is a critical consideration for design. Reinforced GCLs (i.e., needle-punched and stitch-bonded) are needed for designs on slopes, with the needle-punched variety now being the more common choice. Textured GMs are likewise needed, as opposed to their smooth counterparts, for slope applications. Both the internal shear strength of a GCL and the interface shear strengths between a GCL and adjacent materials must be considered for stability analysis. Improvements in the internal shear strength of reinforced GCLs have increased the likelihood for interface shear failures, especially at low normal stress, as illustrated by failures observed at the Cincinnati GCL test plots (Daniel et al. 1998). Although laboratory tests have shown that failure of a composite liner may occur internally within a needle-punched GCL as normal stress increases (Byrne 1994; Gilbert et al. 1996), there are no known cases of internal shear failure of needle-punched GCLs in the field.

Fox et al. (1998) presented the results of a comprehensive study of the internal shear strength of adhesive-bonded, stitch-bonded, and needle-punched GCLs. In this paper, a follow-up study is presented on the interface shear strength between smooth and textured high density polyethylene (HDPE) geomembranes and a needle-punched GCL. This combination is the most common GCL composite liner currently used in landfill construction. Laboratory tests were performed using a large direct shear machine capable of measuring peak and large displacement (200 mm) shear strengths. Testing procedures are described and results are presented for each GM/GCL interface. The results of separate studies on the effects of displacement rate, GM shear direction, and interface material damage on measured shear strength are also presented.

As with GCL internal shear strength, measured values of GM/GCL interface shear strength are dependent on many factors, including product type, hydration and shear conditions, and specifics of the equipment used to perform the tests (e.g., specimen gripping system). Shear strength information presented in this paper may be useful for preliminary design purposes and to gain insight into GM/GCL interface behavior. However, design values of GM/GCL interface shear strength must be measured on a product-specific basis under conditions closely simulating those expected in the field.

LABORATORY TESTING PROGRAM

Materials

Six GM/GCL interfaces, described in Table 1, were tested in this study. Tests were conducted using both sides of one reinforced GCL product (Bentomat ST, Colloid Environmental Technologies Co., Arlington Heights, IL) having a nominal minimum mass/area of 3.7 kg/m² at zero water content. Granular bentonite is held between a woven (W) slit-film polypropylene geotextile (109 g/m²) and a nonwoven (NW) needle-punched polypropylene geotextile (204 g/m²). To provide reinforcement, polypropylene fibers from the nonwoven geotextile are needle-punched through the bentonite and the wo-

TABLE 1. GM/GCL Interfaces Tested for Experimental Program

GM/GCL interface	Geomembrane	Geosynthetic clay liner
SM/W	Smooth HDPE (40 mil)	Woven geotextile of woven/nonwoven needle-punched GCL
SM/NW	Smooth HDPE (40 mil)	Nonwoven geotextile of woven/nonwoven needle-punched GCL
LM/W	Laminated textured HDPE (40 mil)	Woven geotextile of woven/nonwoven needle-punched GCL
LM/NW	Laminated textured HDPE (40 mil)	Nonwoven geotextile of woven/nonwoven needle-punched GCL
CX/W	Coextruded textured HDPE (40 mil)	Woven geotextile of woven/nonwoven needle-punched GCL
CX/NW	Coextruded textured HDPE (40 mil)	Nonwoven geotextile of woven/nonwoven needle-punched GCL

¹Staff Engr., Geosyntec Consultants, Atlanta, GA 30342.

²Assoc. Prof., Dept. of Civ. and Envir. Engrg., Univ. of California, Los Angeles, CA 90095.

Note. Discussion open until November 1, 2001. To extend the closing date one month, a written request must be filed with the ASCE Manager of Journals. The manuscript for this paper was submitted for review and possible publication on April 28, 2000; January 16, 2001. This paper is part of the *Journal of Geotechnical and Geoenvironmental Engineering*, Vol. 127, No. 6, June, 2001. ©ASCE, ISSN 1090-0241/01/0006-0543-0552/\$8.00 + \$.50 per page. Paper No. 22168.

ven geotextile. Peel tests were performed on 102×254 mm GCL specimens in their as-received moisture condition at a displacement rate of 305 mm/min using a procedure similar to that specified by ASTM D 4632 for grab strength of geotextiles. The peel strength of the GCL product, taken as the average measured tensile force from 20 peel tests, was 94 N. The coefficient of variation (standard deviation/mean) of peel strength was 28%.

Three 1.0 mm (40 mil) HDPE geomembrane products were sheared against the GCL specimens. The first geomembrane (Dura Seal, National Seal Company, Galesburg, IL), designated "SM," was smooth. The second geomembrane (Friction Seal, National Seal Company), designated "LM," had texturing that was laminated onto a 1.0 mm smooth backing geomembrane. The third geomembrane (HD Textured, GSE Lining Technology, Inc., Houston, Tex.), designated as "CX," was a round-dye coextruded textured product. The textured geomembranes were textured only on one side so that specimens could be effectively glued to the pullout plate of the shear machine (see the next section).

Equipment

Direct shear tests were performed on large ($406 \times 1,067$ mm) rectangular GM/GCL specimens using the pullout shear machine described by Fox et al. (1997). A scale drawing of the machine and specimen configuration is shown in Fig. 1. The machine is capable of shear displacements up to 203 mm under normal stresses ranging from 1 to 486 kPa. Each GM/GCL composite specimen was sheared between a horizontal stainless steel pullout plate and the floor of the test chamber. The lower shearing surface was covered with sharp metal plates that gripped the GCL specimen and permitted it to drain on the bottom. The GM specimen was glued to the underside of the pullout plate. Both shearing surfaces enforced uniform shear strain at failure without clamping the ends of the GM or GCL specimens. Volume change of the GM/GCL specimens was measured during hydration and shear. Pore pressures at

the interface between the GM and GCL were also measured during hydration and shear using a thin stainless steel needle that was embedded in the pullout plate. A small hole was cut in the center of each GM specimen (and sealed with silicone gasket sealant) to permit this measurement.

Procedures

Specimen Hydration and Shear

GCL specimens were hydrated using the four-day, two-stage procedure described by Fox et al. (1998). For the first stage of hydration, each specimen ($406 \times 1,067$ mm) was cut parallel to the machine direction and placed in a shallow pan. The appropriate amount of tap water was then added to bring the specimen to the estimated final water content for the test. These final water content values vary with normal stress and were obtained from previous direct shear tests using the same GCL product (Fox et al. 1998). The specimens were covered to prevent evaporation and allowed to cure for two days under 1 kPa vertical stress. For the second stage of hydration, GCL specimens were placed on the lower shearing surface of the machine with the desired geotextile (woven or nonwoven) facing upward. GM specimens ($406 \times 1,270$ mm) were cut in the machine direction and glued to the pullout plate. An "original" direction of shear was chosen for each textured geomembrane product prior to the start of testing. A water-resistant spray-on adhesive and a two-part epoxy were used to glue the GM specimens for low and high normal stress conditions, respectively. The locations of the ends of each GM were marked on the plate so that any slippage of the GM could be detected and, if such slippage occurred, the test was rejected. Normal stress (σ_v) was applied and the specimens were hydrated for an additional two days.

Once the second stage of hydration was completed, the GM/GCL specimens were sheared to a final displacement of approximately 200 mm at a constant displacement rate of 0.1 mm/min. Additional tests were conducted at 0.01, 1, and 10

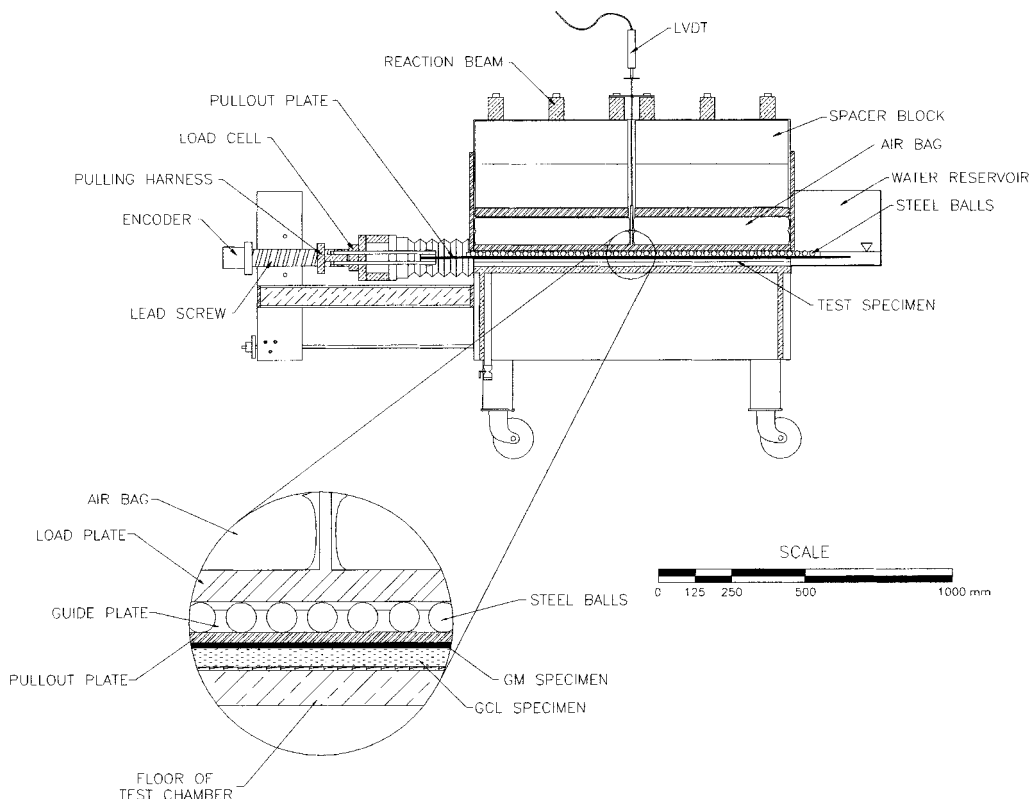


FIG. 1. Pullout Shear Machine

mm/min and at $\sigma_n = 72.2$ kPa to measure the effect of displacement rate on measured interface shear strength. The effect of GM shearing direction on interface shear strength was investigated by performing tests (72.2 kPa, 0.1 mm/min) with textured GM specimens oriented 180° from the “original” shear direction. Mechanisms of postpeak strength reduction were evaluated (72.2 kPa, 0.1 mm/min) using a “reshear” procedure similar to that described by Li (1995) for coextruded textured GM/nonwoven geotextile interfaces. A textured GM/GCL interface was first sheared to 200 mm displacement. A new GM specimen was then placed over the same GCL specimen and sheared to 200 mm. Comparison of data for the two tests indicates the extent of GCL geotextile damage that occurred during shear. After the second test was completed, a new GCL specimen was sheared against the original GM specimen to give a corresponding indication of the extent of GM damage that occurred during shear.

Posttest Measurements

After shearing was completed, the GM/GCL specimens were removed from the machine, the mode of failure was noted, and five water content measurements were taken from each GCL. Textured GM specimens from selected tests were placed in a 105°C oven overnight and the dry weight was recorded. These specimens were then washed with tap water and lightly scrubbed with a plastic bristle brush. The effluent from this process contained bentonite that had extruded to the interfaces and HDPE asperities that had detached from the GM specimens during shear. The effluent was passed through a #100 sieve to capture the HDPE asperities. The GMs were

then returned to the oven overnight and weighed again. Extruded bentonite was also scraped off a representative 305 × 305 mm area of the corresponding GCL specimens and oven dried. The mass per unit area of dry bentonite on the GM/GCL interfaces and the mass per unit area of detached HDPE asperities were calculated from these measurements.

RESULTS

Fifty five direct shear tests were conducted for the experimental program. Table 2 provides a summary of test results for interface shear strength and displacement rate effect. Successful tests for the LM/NW, CX/W, and CX/NW interfaces could not be conducted at $\sigma_n = 486$ kPa due to failure of the epoxy.

Hydration

Fig. 2 shows typical measurements of vertical displacement (i.e., volume change) and interface pore pressure during hydration (LM/W). Using the two-stage hydration procedure, most specimens attained vertical displacement and pore pressure equilibrium within 48 h, and many within 24 h. The specimens hydrated at $\sigma_n = 6.9$ kPa were a notable exception, as the vertical displacement plots indicate continued swelling at the end of hydration. Gilbert et al. (1997) defined a hydration factor as $|h_t - h_{t-12}|/h_t$, where h_t is the GCL thickness at time t (end of hydration) and h_{t-12} is the GCL thickness 12 h before time t . A GCL specimen having a hydration factor less than 5% is considered to be completely hydrated. If the thickness of the GCL specimens at 48 h (which is unknown) is conser-

TABLE 2. Testing Program and Results—Shear Strength and Displacement Rate Effects

GM/GCL interface	Normal stress, σ_n (kPa)	Horizontal displacement rate (mm/min)	Peak shear strength, τ_p (kPa)	Horizontal displacement at peak, δ_p (mm)	Pore pressure at peak (kPa)	Large displacement (200 mm) shear strength, τ_{ld} (kPa)	Pore pressure at large displacement (200 mm) (kPa)
SM/W	6.9	0.1	1.4	0.6	0.2	1.3	0.2
SM/W	72.2	0.1	12.8	0.6	1.4	10.5	1.4
SM/W	141	0.1	25.1	0.9	2.1	20.3	5.5
SM/W	279	0.1	48.4	1.5	8.3	36.3	13.7
SM/W	486	0.1	84.4	2.4	27.6	61.8	37.9
SM/W	72.2	0.01	12.6	0.8	2.1	9.9	1.4
SM/W	72.2	1.0	12.9	0.6	2.8	9.3	4.8
SM/W	72.2	10.0	12.5	0.6	0.7	11.9	0.7
LM/W	6.9	0.1	4.8	9.8	0.1	2.2	0.1
LM/W	72.2	0.1	31.4	18.3	0	18.0	-5.4
LM/W	141	0.1	58.1	9.7	0.8	32.6	-3.2
LM/W	279	0.1	83.6	14.4	31.0	47.2	-2.6
LM/W	486	0.1	138.7	14.3	38.5	72.4	8.3
LM/W	72.2	0.01	36.3	8.8	0.9	19.1	1.6
LM/W	72.2	1.0	30.5	9.7	-0.4	17.3	2.3
LM/W	72.2	10.0	37.7	7.9	-0.7	18.5	3.5
CX/W	6.9	0.1	3.5	8.8	0	1.8	0
CX/W	72.2	0.1	32.2	7.0	0	19.4	0
CX/W	141	0.1	49.9	14.6	2.1	28.2	-0.7
CX/W	279	0.1	123.9	10.0	0.1	60.9	1.5
CX/W	72.2	0.01	29.5	13.0	5.0	18.8	5.6
CX/W	72.2	1.0	24.8	15.7	0.2	16.6	0.2
CX/W	72.2	10.0	29.4	6.4	0.2	15.3	2.1
SM/NW	6.9	0.1	1.7	0.5	0	1.6	-1.3
SM/NW	72.2	0.1	13.1	0.7	0	12.4	0
SM/NW	141	0.1	25.9	1.3	1.5	23.4	0.8
SM/NW	279	0.1	46.9	1.8	16.5	38.4	8.3
SM/NW	486	0.1	85.8	2.5	13.8	64.7	15.2
LM/NW	6.9	0.1	11.4	17.4	0.1	4.6	0.8
LM/NW	72.2	0.1	56.6	12.0	0.1	26.5	1.6
LM/NW	141	0.1	88.4	13.7	0.7	39.5	1.4
LM/NW	279	0.1	181.9	15.3	3.0	67.5	0.9
CX/NW	6.9	0.1	10.8	21.3	0.1	4.7	-1.9
CX/NW	72.2	0.1	45.8	12.8	0	22.8	0
CX/NW	141	0.1	84.1	12.3	1.0	39.2	-0.3
CX/NW	279	0.1	157.5	12.2	2.8	61.9	-0.6

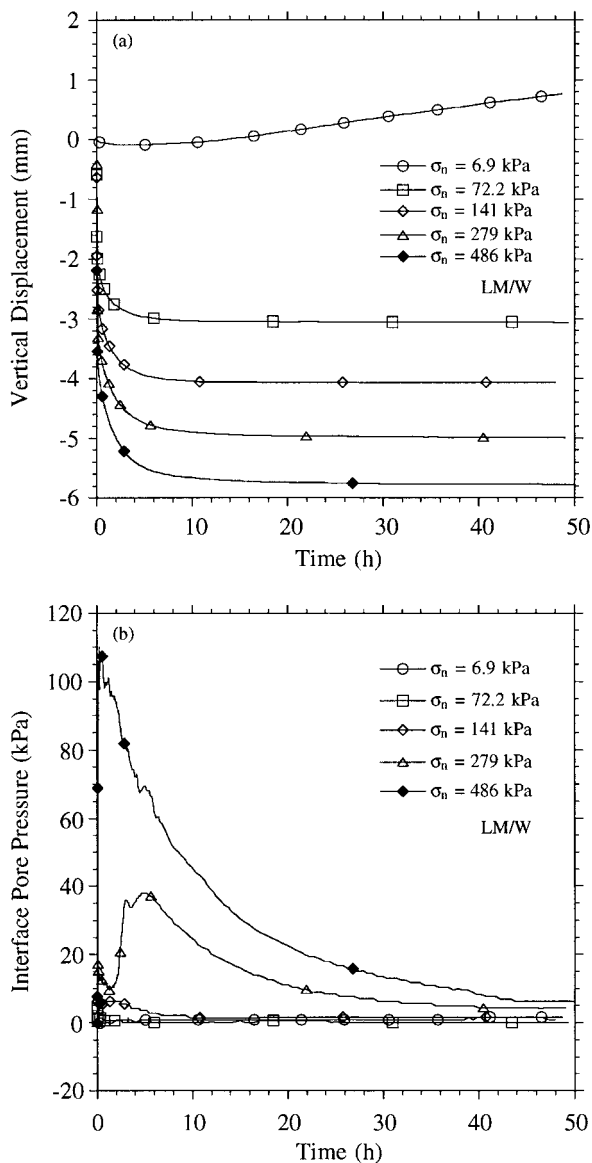


FIG. 2. LM/W during Second-Stage Hydration: (a) Vertical Displacement; (b) Interface Pore Pressure

vatively assumed to be a constant 5 mm, then the hydration factor is less than 5% for all tests except CX/NW at $\sigma_n = 6.9$ kPa (which had a hydration factor of 9%). Excluding the tests at $\sigma_n = 6.9$ kPa, values of hydration factor range from 0 to 0.4%. The two-stage hydration procedure was thus effective in reducing the required in-machine hydration time from a typical 10–20 days (Gilbert et al. 1997) to 2 days. Pore pressure data also shows that equilibrium was typically achieved in 48 h using the procedure.

Stress-Displacement Behavior

Shear stress (τ) versus horizontal displacement (δ) curves for the six types of GM/GCL specimens are shown in Fig. 3. Each failure occurred at the GM/GCL interface (i.e., no internal GCL failures were observed). Most curves display marked postpeak strength reduction from peak shear strength (τ_p) to large displacement shear strength (τ_{ld}) at $\delta = 200$ mm. The large displacement shear strengths are not residual strengths, for which no further decrease occurs with additional displacement. Considering published ring-shear data on HDPE GM/nonwoven geotextile interfaces (Stark et al. 1996), displacements of approximately 500–750 mm would likely be needed

to reach residual conditions for the interfaces tested in this study.

The large displacement strength ratio (τ_{ld}/τ_p) for each interface is plotted versus σ_n in Fig. 4. The ratio for the smooth GM interfaces decreased with increasing normal stress to a minimum value of 0.73 at $\sigma_n = 486$ kPa, with the SM/W interfaces yielding consistently lower values than the SM/NW interfaces. The textured GM interfaces experienced more strength reduction, with τ_{ld}/τ_p values ranging from 0.61 to 0.37. Interestingly, the τ_{ld}/τ_p ratio for each textured GM interface reached a maximum at $\sigma_n = 72.2$ kPa. Also, unlike the results for the smooth GM, nonwoven geotextile interfaces experienced the most postpeak strength reduction for the textured GMs. Strength reduction was slightly more for the LM product than for the CX product.

Fig. 5 shows horizontal displacement at peak strength (δ_p) versus σ_n for each interface. Values of δ_p for the smooth GM were small, less than 3 mm, and increased steadily with increasing normal stress. Larger displacements, 7–21 mm, were needed to reach peak strength for the textured GM interfaces. The data for these tests show no clear trend between δ_p and σ_n .

Measured values of interface pore pressure at peak and large displacement shear strengths are shown in Fig. 6. Pore pressures generally increased with increasing normal stress and were higher for the smooth GM interfaces. With the exception of the LM/W interface, small pore pressures were recorded for the textured GM interfaces. The maximum ratio of interface pore pressure at τ_p to normal stress was 0.11. Interface pore pressure measurements can only be expected to indicate qualitative trends due to the lack of back pressure in this study.

Shear Strength

Peak shear strengths are plotted versus total normal stress in Fig. 7(a). Each failure envelope, with the exception of LM/W, is approximately linear and is characterized using

$$\tau_p = c_p + \sigma_n \tan \phi_p \quad (1)$$

where c_p and ϕ_p are cohesion intercept and interface friction angle, respectively, determined from linear regression. The LM/W envelope is approximately bilinear and is characterized using (1) fitted to each segment individually. Table 3 lists peak shear strength parameters and their applicable stress range for each interface. Differences in peak strength failure envelopes based on total normal stresses and effective normal stresses [calculated using pore pressures in Fig. 6(a)] are minor, with effective stress envelopes yielding slightly higher interface friction angles due to the positive pore pressures measured at peak strength (Triplett 1998).

The SM/W and SM/NW interfaces had nearly identical peak strengths at all stress levels. The resulting ϕ_p value of 9.8° is larger than the value of $\phi_p = 8.4^\circ$ reported by Gilbert et al. (1996) for similar materials. Peak shear strengths for the textured GM/nonwoven interfaces were consistently higher than those measured for the textured GM/woven interfaces. Differences in peak strength for the two textured GM products sheared against the nonwoven GCL geotextile were relatively minor, with the strength of the LM/NW interface approximately 10–15% higher than that for the CX/NW interface. A different behavior was observed for the textured GM/woven geotextile interfaces. The LM/W and CX/W interfaces had similar peak strengths for normal stresses up to 141 kPa. The failure envelopes then diverge at higher normal stresses, with LM/W yielding lower shear strengths and a bilinear envelope.

Fig. 7(a) also shows the internal peak strength failure envelope for the same needle-punched GCL product as presented by Fox et al. (1998). The peel strength of this material was 85 N, which is lower than the value of 94 N for the GCL material

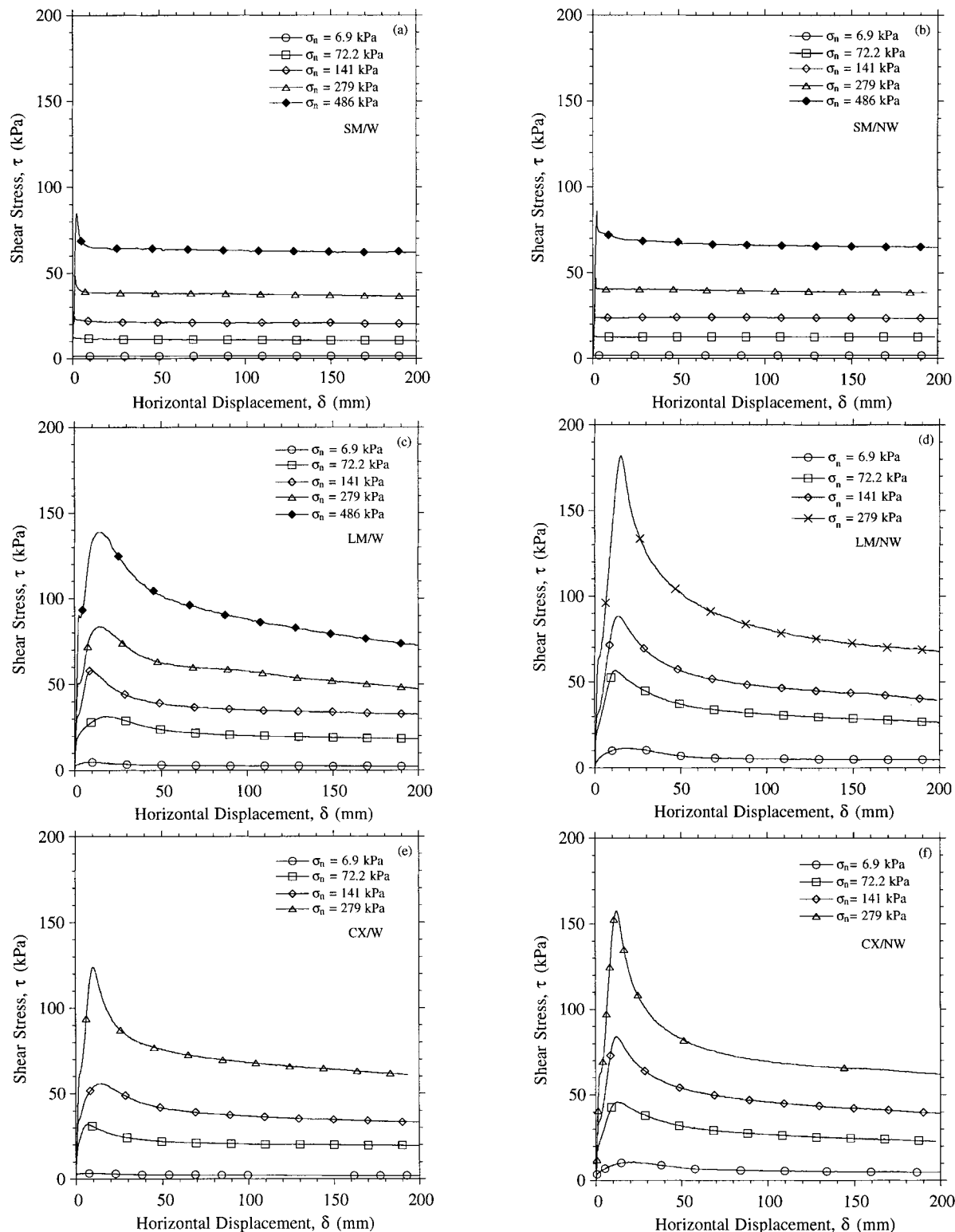


FIG. 3. Stress-Displacement Curves for: (a) SM/W; (b) SM/NW; (c) LM/W; (d) LM/NW; (e) CX/W; (f) CX/NW

used in the current study. The failure envelope for the GCL material used in the current study would therefore be expected to be somewhat higher than the envelope shown in Fig. 7(a). Peak shear strength values for all interfaces are substantially less than the peak strength of the GCL itself. This is consistent with the observation that all failure planes were located at the interfaces and none were located within the GCL.

Large displacement (200 mm) failure envelopes, each approximated as bilinear, are shown in Fig. 7(b). Large displacement shear strength parameters were obtained using

$$\tau_{ld} = c_{ld} + \sigma_n \tan \phi_{ld} \quad (2)$$

and are provided in Table 3. Large displacement failure envelopes based on total and effective normal stresses [calculated using pore pressures in Fig. 6(b)] again show minor differences (Triplett 1998). The envelopes follow trends with respect to normal stress and interface type that are similar to those in Fig. 7(a). The difference between shear strengths of smooth and textured GM interfaces at $\delta = 200$ mm is considerably less than corresponding differences at peak strength, presum-

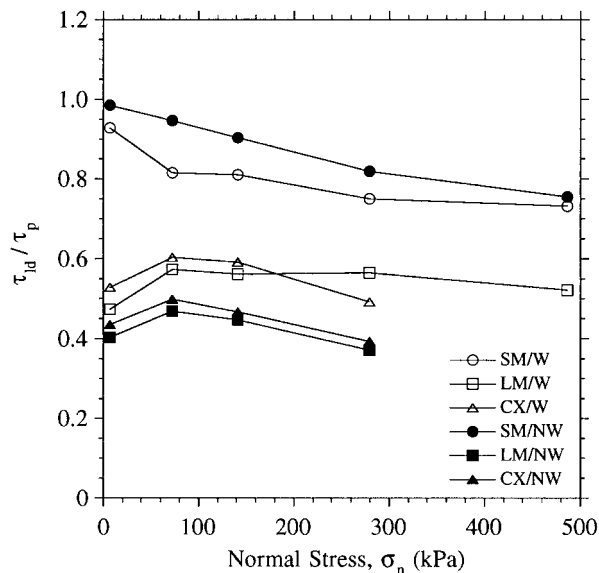


FIG. 4. τ_{id}/τ_p for GM/GCL Interfaces

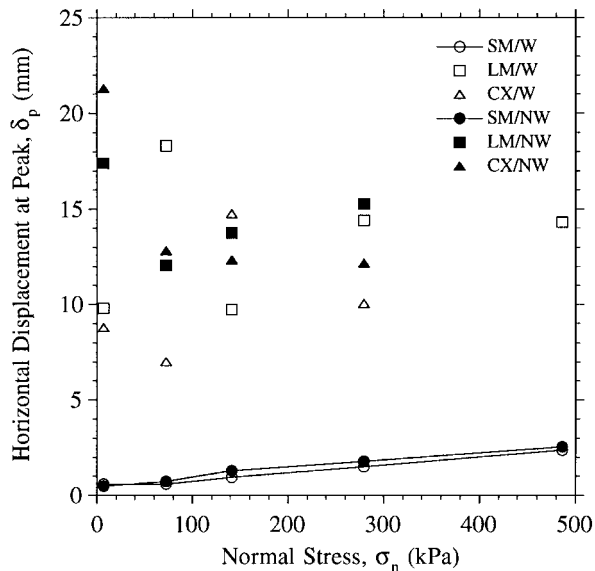


FIG. 5. Horizontal Displacements at τ_p for GM/GCL Interfaces

ably due to higher levels of damage that occur for textured GM interfaces.

The internal residual strength failure envelope for the GCL (Fox et al. 1998) is also shown in Fig. 7(b). Considering that residual shear strength does not vary with peel strength, the GCL failure envelope shown in Fig. 7(b) should represent a close approximation for the GCL material in the current study. With the exception of the SM/W and SM/NW interfaces at $\sigma_n = 6.9$ kPa, τ_{id} values for all interfaces exceed the residual shear strength of the GCL. Thus, if the GCL specimens had failed internally, all values of τ_{id} would have been controlled by the residual shear strength of the hydrated bentonite.

Although failure envelopes were approximated as linear or bilinear in the current study, it is recognized that a nonlinear model may be more appropriate over large stress ranges. To illustrate, Fig. 8 shows τ_p for the LM/W interface at low normal stress. The plot includes data from one additional test at $\sigma_n = 1$ kPa. The failure envelope is curved at low normal stress and passes essentially through the origin. This suggests that nonlinear models having a zero cohesion intercept, while inappropriate for the internal strength of reinforced GCLs, are appropriate for GM/GCL interface shear strength. The general

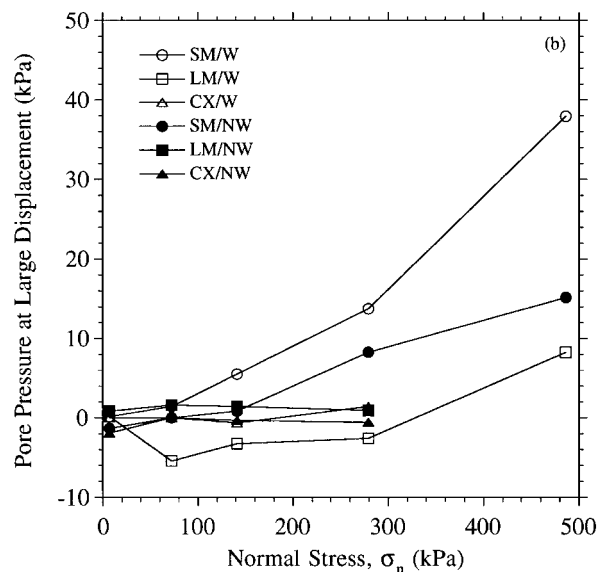
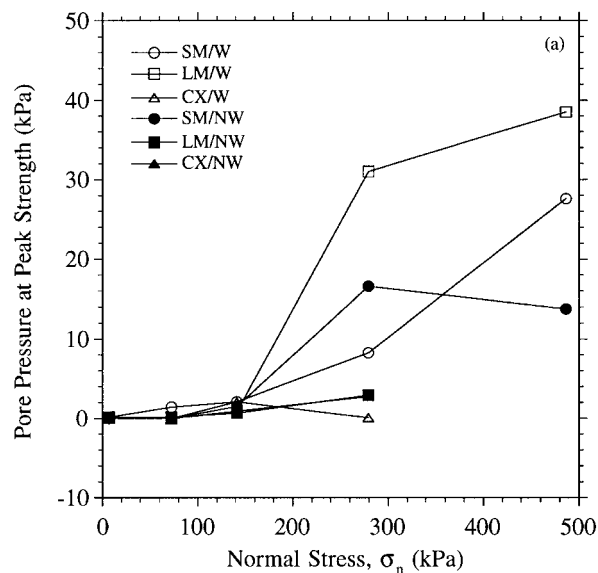


FIG. 6. Interface Pore Pressures at: (a) Peak Shear Strength; (b) Large Displacement Shear Strength

nonlinearity of failure envelopes underscores the need to report applicable normal stress ranges with interface strength parameters obtained using linear equations [also emphasized by Stark (1997)].

Effect of Displacement Rate

The effect of horizontal displacement rate on peak and large displacement shear strengths of the SM/W, LM/W, and CX/W interfaces ($\sigma_n = 72.2$ kPa) is shown in Fig. 9. Although the test data show variability, especially for the textured GM interfaces, no consistent trend is observed between displacement rate and measured shear strength. This finding is in agreement with previously published data indicating that the shear strength of a textured GM/nonwoven geotextile interface is independent of displacement rate (Stark et al. 1996).

Effect of Geomembrane Shear Direction

The effect of geomembrane specimen orientation on measured shear strength is shown for the LM/W and CX/W interfaces ($\sigma_n = 72.2$ kPa) in Fig. 10. Textured GM specimens sheared in the "original" direction generally yielded higher peak shear strengths, by 12% on average, than specimens

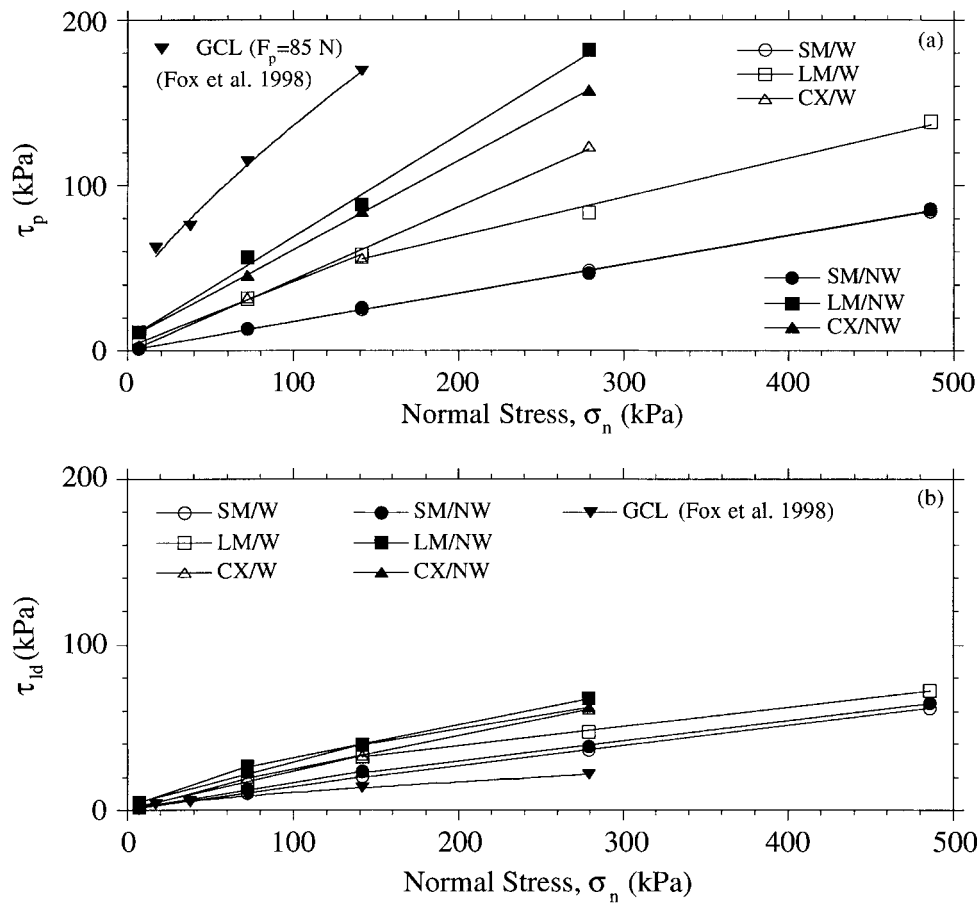


FIG. 7. Failure Envelopes for: (a) Peak Shear Strength; (b) Large Displacement Shear Strength

TABLE 3. Peak and Large Displacement Shear Strength Parameters

GM/GCL interface	Normal stress range σ_n (kPa)	Peak Strength Parameters		Normal stress range σ_n (kPa)	Large Displacement (200 mm) Strength Parameters	
		c_p (kPa)	ϕ_p (degrees)		c_{ld} (kPa)	ϕ_{ld} (degrees)
SM/W	6.9–486	0.3	9.8	6.9–127	0.3	8.1
				127–486	3.0	6.9
LM/W	6.9–124	2.2	21.6	6.9–134	1.0	12.7
	124–486	22.0	13.3	134–486	15.7	6.6
CX/W	6.9–279	0	23.7	6.9–71.9	0	15.0
				71.9–279	4.9	11.3
SM/NW	6.9–486	0.4	9.9	6.9–127	0.6	9.2
				127–486	5.8	6.9
LM/NW	6.9–279	7.4	31.7	6.9–69.6	2.3	18.5
				69.6–279	11.8	11.2
CX/NW	6.9–279	7.2	28.3	6.9–135	3.4	14.4
				135–279	16.0	9.3

tested in the “reverse” direction (i.e., 180° from the “original” direction). Variability of the test results in Fig. 10 is attributed to GCL product variability, as GCL specimens were taken from several rolls with different peel strengths. In general, interface shear strength between the woven geotextile side of the GCL and a textured GM was found to increase with increasing GCL peel strength. Higher peel strengths correspond to a greater density of needle-punched reinforcing fibers that protrude through the woven geotextile of the GCL and increase the interface shear resistance. Interface shear strength with the nonwoven side of the GCL would be expected to show less variability because the surface texture of the nonwoven geo-

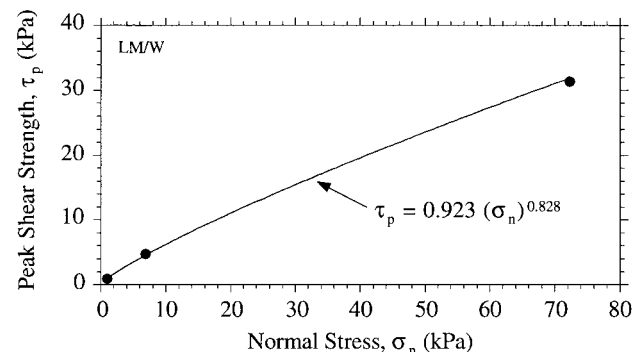


FIG. 8. Peak Shear Strength Failure Envelope for LM/W at Low Normal Stress

textile does not vary as much with the density of needle-punched fibers.

Bentonite Extrusion and Geomembrane Asperity Removal

The total mass/area of bentonite removed from the textured GMs and the surfaces of the corresponding GCL specimens ranged from 12 to 38 g/m² (dry weight basis). Although the data is limited, the quantity of extruded bentonite generally increased with increasing normal stress and was less for nonwoven geotextile interfaces than for woven geotextile interfaces, trends also observed in swell tests by Stark (1997). Lesser amounts of extruded bentonite were observed along interfaces with the smooth GM, possibly because the smooth GM allowed less interface drainage than did the textured GMs. Bentonite extrusion on textured GM/GCL (woven geotextile) interfaces has also been observed after shear failures in the

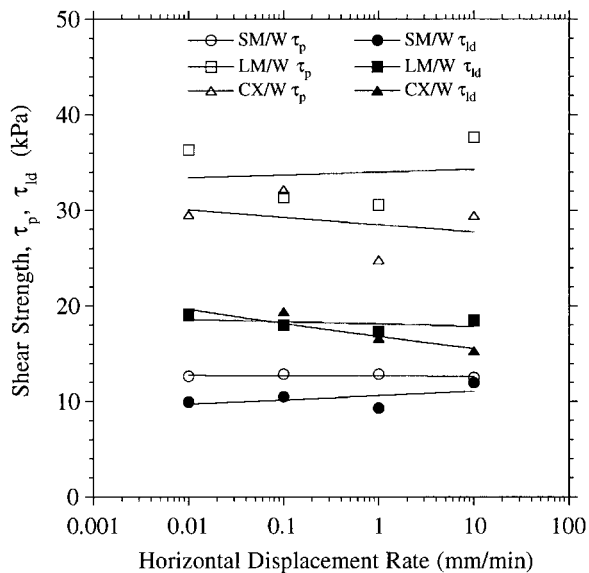


FIG. 9. Effect of Horizontal Displacement Rate on Shear Strength of GM/GCL Interfaces

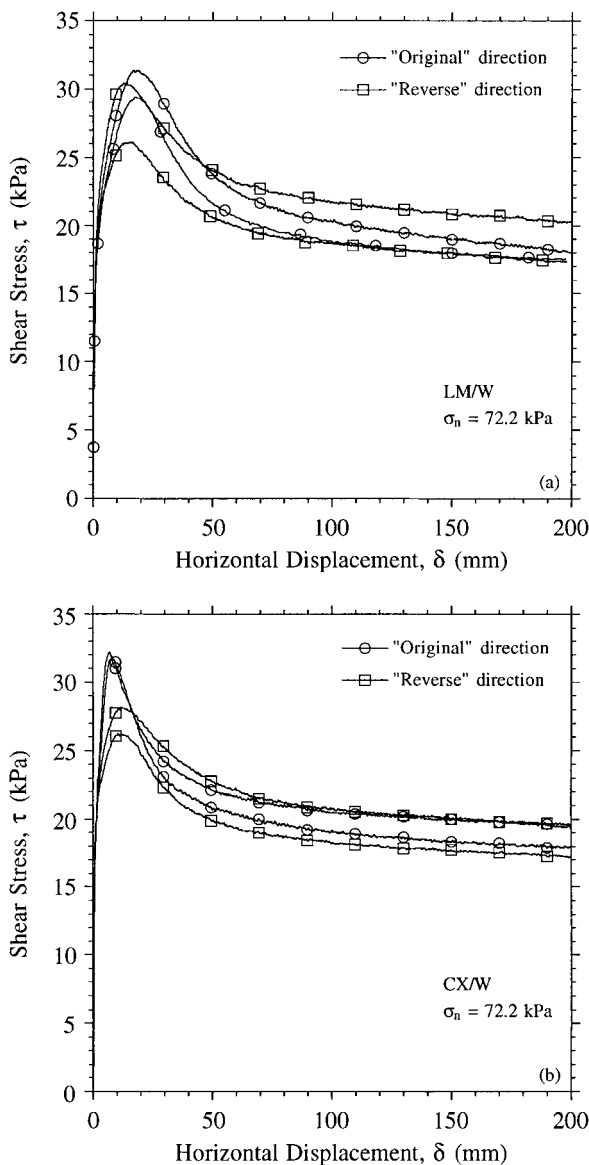


FIG. 10. Effect of GM Shear Direction on Stress-Displacement Curves for: (a) LM/W; (b) CX/W

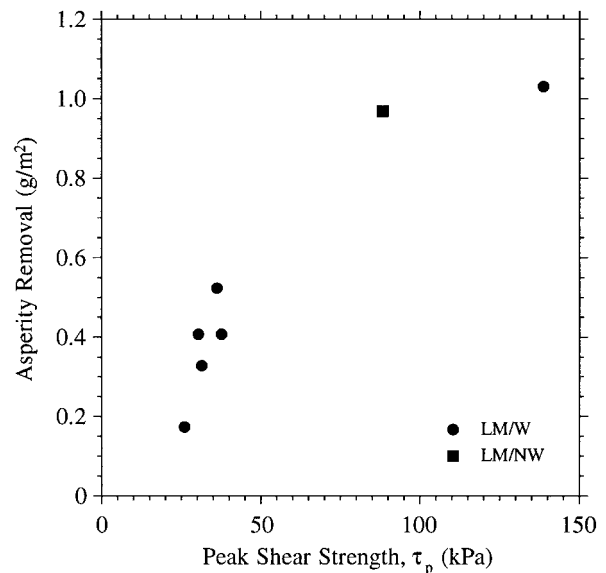


FIG. 11. Asperity Removal versus Peak Shear Strength for LM Geomembrane

laboratory (Gilbert et al. 1996; Stark and Eid 1996) and in field tests (Daniel et al. 1998).

Each specimen of the LM product that was washed after shearing showed removal of asperities, with amounts ranging from 0.2 to 1.0 g/m² [similar observations were made by Stark et al. (1996)]. Asperity removal increased with increasing normal stress and showed a nonlinear correlation with peak shear strength (Fig. 11). Asperity removal was not observed for specimens of the CX product under any normal stress.

Material Damage during Shear

Considering that small amounts of extruded bentonite were measured at the various interfaces in this study, postpeak strength reduction probably occurred largely as a result of damage to the geosynthetic materials. Damage mechanisms for a GM involve polishing and removal of asperities, whereas GCL damage mechanisms involve polishing, breakage, pull-out, and alignment of geotextile fibers.

The effects of previous GM or GCL shearing on subsequent stress-displacement behavior are shown for each textured GM interface ($\sigma_n = 72.2$ kPa) in Fig. 12. Relative levels of GM and GCL damage that occurred during shear can be inferred from these results. Previous shearing (to 200 mm) of either the GM or GCL specimen reduced subsequent peak shear strengths by 11–32%. Tests for the LM/W interface show that previous shear of the GCL specimen resulted in a lower subsequent peak strength than previous shear of the GM specimen. This suggests that GCL damage makes a larger contribution to postpeak strength reduction than GM damage for this interface. The reverse occurred for the LM/NW interface, in which GM damage appears to be the controlling mechanism with regard to postpeak strength reduction. Larger amounts of GM damage would be expected for the LM/NW interface due to the higher shear strength and the likelihood for greater asperity removal.

Tests for the CX product interfaces show little difference in subsequent peak strength regardless of which material was previously sheared, suggesting that GM and GCL damage contribute equally to postpeak strength reduction at $\sigma_n = 72.2$ kPa. Gilbert and Byrne (1996) concluded that GM damage was the largest contributor to shear strength reduction for coextruded GM/nonwoven geotextile interfaces tested at $\sigma_n = 690$ kPa. Clearly, relative amounts of material damage are expected to be product-specific and dependent on normal stress level.

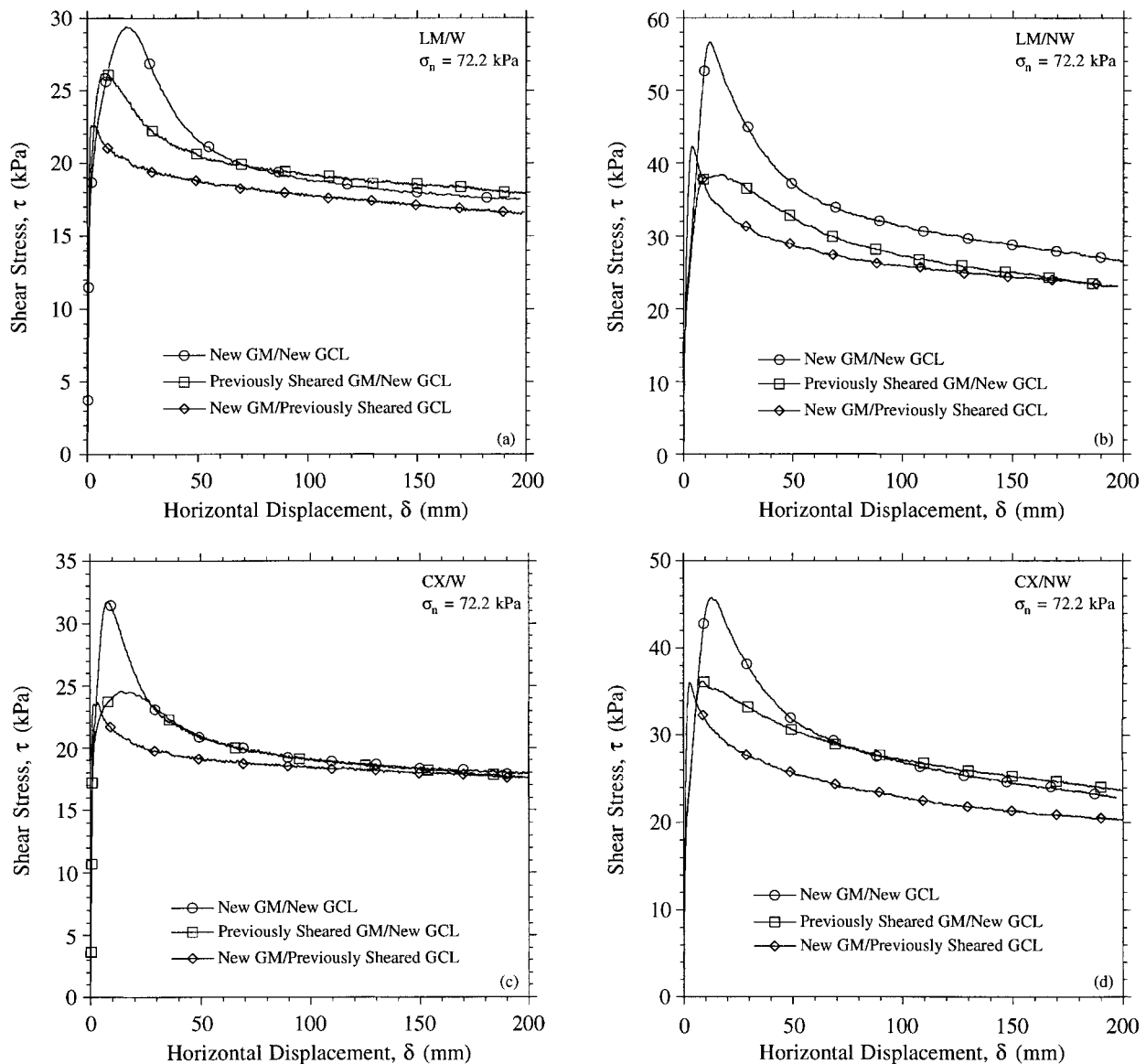


FIG. 12. Effect of Previous GM and GCL Shearing on Stress-Displacement Curves for: (a) LM/W; (b) LM/NW; (c) CX/W; (d) CX/NW

The plots in Fig. 12 consistently show that peak shear strength was reached at a smaller horizontal displacement when the GCL was sheared previously. A similar conclusion was reached by Li (1995) for coextruded GM/nonwoven geotextile interfaces. This suggests that interface shear stiffness and displacement at peak strength are primarily related to physical changes of the GCL geotextile (such as fiber reorientation) that occur during shear.

CONCLUSIONS

The following conclusions are reached as a result of this investigation of interface shear strengths between smooth (SM), laminated (LM), and coextruded (CX) HDPE geomembranes (GMs) and a needle-punched geosynthetic clay liner (GCL) having woven (W) and nonwoven (NW) carrier geotextiles:

1. Long periods of hydration and very slow shearing rates are probably not needed for GM/GCL interface strength tests. Tests may be accelerated using a two-stage hydration procedure similar to that described in this paper and shearing at the maximum rate of 1 mm/min specified by ASTM D 6243.
2. The failure surface was located at the GM/GCL interface for all tests conducted, corresponding to a normal stress (σ_n) range of 1–486 kPa. No internal GCL failures were observed. The average peel strength for the GCL product was 94 N.
3. Postpeak strength reduction was measured for all interfaces. The maximum strength loss for smooth GM interfaces was 27% of peak shear strength (τ_p). Textured GM interfaces experienced larger strength losses, with values ranging from 39 to 63% of τ_p .
4. Relatively small positive pore pressures were measured for all interfaces at τ_p . This suggests that the practice of preparing failure envelopes based on total normal stress, instead of effective normal stress, is conservative. Uncertainty with regard to interface pore pressures developed during shear remains a significant issue for testing and design. Interface pore pressure measurements can only indicate qualitative trends due to the lack of back pressure in this study.
5. Horizontal displacements of less than 3 mm were required to reach τ_p for the smooth GM interfaces. Larger displacements, 7–21 mm, were needed to reach τ_p for the textured GM interfaces.
6. Peak shear strength failure envelopes were approxi-

mated as linear or bilinear for the normal stress range tested. Envelopes for the SM/W and SM/NW interfaces were nearly identical. Peak strengths for textured GMs placed against the NW side of the GCL were consistently higher than those corresponding to the W side. LM/NW interfaces were stronger than CX/NW interfaces, whereas peak strengths of the LM/W and CX/W interfaces were comparable for $\sigma_n \leq 141$ kPa and then diverged for $\sigma_n > 141$ kPa.

7. Large displacement (200 mm) shear strength (τ_{ld}) failure envelopes were approximated as bilinear. With the exception of the SM/W and SM/NW interfaces at $\sigma_n = 6.9$ kPa, τ_{ld} values for all interfaces exceed the residual shear strength of the GCL.
8. Peak shear strengths for the LM/W and CX/W interfaces were dependent on the shear direction of the GM. At $\sigma_n = 72.2$ kPa, τ_p varied by an average factor of 1.12 for GM specimens sheared in opposite directions. Since it may not be possible to control the deployment direction of GM rolls in the field, replicate shear tests with textured GM specimens placed in opposite directions may be needed to obtain conservative design parameters.
9. The quantity of extruded bentonite at the interfaces generally increased with normal stress and was less for nonwoven geotextile interfaces than for woven geotextile interfaces. Lesser amounts of extruded bentonite were observed along interfaces with the smooth GM.
10. The shearing process removed asperities from the LM product but not for the CX product. A nonlinear correlation was found between τ_p and asperity removal for interface shear tests conducted using the LM product.
11. Contributions of GM and GCL damage to postpeak strength reduction were found to be roughly equivalent for textured GM interfaces at $\sigma_n = 72.2$ kPa.

Shear strength behavior of the textured GM/GCL interfaces in this study is similar to published test data for GMs sheared against woven and nonwoven geotextiles. The principal differences between GM/geotextile interface strength and GM/GCL interface strength results from the presence of extruded bentonite at the interface and the effect of GCL needle-punching on shear resistance. Bentonite extrusion and needle-punching probably do not significantly alter interface shear strength on the nonwoven side of the GCL. On the woven side, bentonite extrusion and needle-punching probably act to decrease and increase interface shear strength, respectively, although the net result of these two effects is currently unknown. As such, a correlation may exist between the peel strength of a woven/nonwoven needle-punched GCL and the interface shear strength for textured GMs placed against the woven side.

ACKNOWLEDGMENTS

This investigation was financially supported by the Colloid Environmental Technologies Co. (CETCO) and Grant No. CMS-9622644 from the Geomechanical, Geotechnical, Geoenvironmental Systems Program of the U.S. National Science Foundation. This financial support is gratefully acknowledged. The direct shear tests were conducted in the Bechtel Geotechnical Laboratory at Purdue University. Rolls of GCL, SM and

LM geomembrane, and CX geomembrane were donated by CETCO, the National Seal Co., and GSE Lining Technology, Inc., respectively. Samples of the two-part epoxy "PolyBond 33" were donated by the Nbond Co. of Cave Creek, AZ. The writers thank Mark Bradford, Robert Kim, Cary Lange, and David Runser for their assistance with the experimental program, as well as Richard Carriker and Jim Olsta of CETCO for their support and assistance with the project. Our thanks also go to John Scheithe for preparing Fig. 1. The views expressed in this paper are solely those of the writers and no endorsement of the sponsors is implied.

REFERENCES

- ASTM. (1999). "Standard test method for grab breaking load and elongation of geotextiles." *ASTM D 4632*, West Conshohocken, Pa.
- ASTM. (1999). "Standard test method for determining the internal and interface shear resistance of geosynthetic clay liner by the direct shear method." *ASTM D 6243*, West Conshohocken, Pa.
- Bryne, R. J. (1994). "Design issues with strain-softening interfaces in landfill liners." *Proc., Waste Tech '94*, Charleston, S.C., 1–26.
- Daniel, D. E., Koerner, R. M., Bonaparte, R., Landreth, R. E., Carson, D. A., and Scranton, H. B. (1998). "Slope stability of geosynthetic clay liner test plots." *J. Geotech. and Geoenviron. Engrg.*, ASCE, 124(7), 628–637.
- Fox, P. J., Rowland, M. G., Scheithe, J. R., Davis, K. L., Supple, M. R., and Crow, C. C. (1997). "Design and evaluation of a large direct shear machine for geosynthetic clay liners." *Geotech. Testing J.*, 20(3), 279–288.
- Fox, P. J., Rowland, M. G., and Scheithe, J. R. (1998). "Internal shear strength of three geosynthetic clay liners." *J. Geotech. and Geoenviron. Engrg.*, ASCE, 124(10), 933–944.
- Gilbert, R. B., and Bryne, R. J. (1996). "Strain-softening behavior of waste containment system interfaces." *Geosynthetics Int.*, 3(2), 181–203.
- Gilbert, R. B., Fernandez, F., and Horsfield, D. W. (1996). "Shear strength of reinforced geosynthetic clay liner." *J. Geotech. Engrg.*, ASCE, 122(4), 259–266.
- Gilbert, R. B., Scranton, H. B., and Daniel, D. E. (1997). "Shear strength testing for geosynthetic clay liners." *Testing and acceptance criteria for geosynthetic clay liners*, L. W. Well, ed., ASTM, West Conshohocken, Pa., 121–135.
- Li, M. H. (1995). "Strength of textured geomembrane and nonwoven geotextile interfaces." MS thesis, University of Texas, Austin, Tex.
- Stark, T. D. (1997). "Effect of swell pressure on GCL cover stability." *Testing and acceptance criteria for geosynthetic clay liners*, L. W. Well, ed., ASTM, West Conshohocken, Pa., 30–44.
- Stark, T. D., and Eid, H. T. (1996). "Shear behavior of reinforced geosynthetic clay liners." *Geosynthetics Int.*, 3(6), 771–786.
- Stark, T. D., Williamson, T. A., and Eid, H. T. (1996). "HDPE geomembrane/geotextile interface shear strength." *J. Geotech. Engrg.*, ASCE, 122(3), 197–203.
- Triplett, E. J. (1998). "Geomembranes/geosynthetic clay liner interface shear strength behavior." MS thesis, Purdue University, West Lafayette, Ind.

NOTATION

The following symbols are used in this paper:

- c_{ld} , ϕ_{ld} = large displacement (200 mm) shear strength parameters;
- c_p , ϕ_p = peak shear strength parameters;
- δ = horizontal displacement;
- δ_p = horizontal displacement at peak strength;
- σ_n = normal stress;
- τ = shear stress;
- τ_{ld} = large displacement (200 mm) shear strength; and
- τ_p = peak shear strength.